Constraint Maps and Free Boundaries

Alessio Figalli * André Guerra † Sunghan Kim ‡ Henrik Shahgholian §

January 17, 2025

1 A brief history of free boundaries

Free boundary problems emerge in various fields of partial differential equations. These problems occur when the behavior of variables changes abruptly at certain values. Numerous examples abound, such as the solid-liquid interface during material solidification, the boundary between exercise and continuation regions of a financial instrument (like an American option), and the transition from elastic to plastic behavior when stress surpasses a critical threshold. These applications often lead to free boundary problems being referred to as phase transition problems.

Classically, mathematical modeling of free boundaries emerged in studying minimal surfaces under constraints, and can be traced back to J.D. Gergonne [Ger16], who in 1816 proposed the following problem:

> *Couper un cube en deux parties, de telle manière que la section vienne se terminer aux diagonales inverses de deux faces opposées, et que l'aire de cette section, terminée à la surface du cube, soit un minimum.*

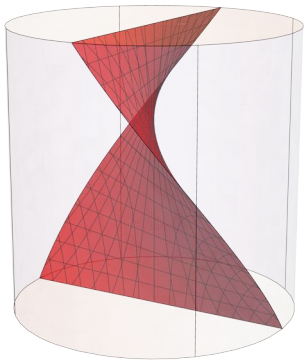


Figure 1: The solution to Gergonne's problem in the case where we cut a cylinder, rather than a cube, in half.

In short, this says: "Cut a cube into two parts so that the section ends at opposite diagonals of two opposite faces, and minimize the area of this section." This problem remained untouched for almost half a century, until Schwarz in 1872 took on studying it, see [Sch72].

In fact, in practical applications, the above type of ideas dates back to Roman times, when ancient architects and engineers utilized principles of minimal surfaces to construct stable and efficient structures like arches and domes. These applications focused on optimizing materials and forms to achieve structural stability, indirectly relating to minimizing surfaces under constraints.

In this survey we will focus on a specific but remarkably ubiquitous family of free boundary problems, those of **obstacle-type**. We will recount the historical development of the topic together with more recent advances, focusing in particular on

*Alessio Figalli is a professor at Department of Mathematics, ETH Zürich. His email address is alessio.figalli@math.ethz.ch.

†André Guerra is a Junior Fellow at the Institute for Theoretical Studies, ETH Zürich. His email address is andre.guerra@eth-its.ethz.ch.

‡Sunghan Kim is a postdoc at Department of Mathematics, Uppsala University. His email address is sunghan.kim@math.uu.se.

§Henrik Shahgholian is a professor at Department of Mathematics, KTH Royal Institute of Technology. His email address is henriksh@kth.se.

vector-valued variational problems with constraints. Our discussion is shaped by the contributions of several distinguished mathematicians working at the intersection of free boundary problems, harmonic maps, and geometric partial differential equations.

2 The scalar obstacle problem

The obstacle problem is a prominent and perhaps the most widely studied type of free boundary problem. Its theoretical advancements have led to progress in numerous other problems in both applied sciences and theoretical research.

To frame the obstacle problem in a mathematical context, consider a simple model of the deformation of an n-dimensional membrane in $\mathbb{R}^{n+1}$, keeping in mind the physical description for $n = 2$. We prescribe the deformation of the membrane on its boundary, and we require the membrane to lie above a given obstacle. For simplicity, we consider the idealized situation in which the membrane is a homogeneous plate of infinite thickness, which does not have resistance, and in which the only acting force is tension[1]. We also assume that the deformation of the membrane is prescribed on its boundary. The solution of the obstacle problem then describes the equilibrium configuration of the membrane under the above constraints.

Let us now give a mathematical formulation of the above problem. Denote by

$$x_{n+1} = u(x), \quad x = (x_1, \cdots, x_n) \in \overline{\Omega}, \tag{2.1}$$

the deformation representing the equilibrium configuration of the membrane, which we assume to be represented as the graph of a function u defined over the closure of a bounded smooth domain $\Omega \subset \mathbb{R}^n$. Since the deformation is prescribed on the boundary, we have

$$u(x) = g(x), \quad x \in \partial\Omega, \tag{2.2}$$

for some given function $g\colon \partial\Omega \to \mathbb{R}$, which we assume to be smooth. For an ideal membrane such as the one we described, the potential energy $\mathcal{P}$ of the deformation is proportional to the increase in area of the surface of the membrane, i.e.

$$\mathcal{P} = (S_1 - S_0),$$

where S_0, S_1 are the surface areas of the membrane before and after the deformation, respectively; for simplicity, we have set the constant of proportionality to be one. We thus have that $S_0 = \text{volume}(\Omega)$ and, from basic Calculus,

$$S_1 = \int_\Omega \sqrt{1 + |Du(x)|^2}\, dx.$$

From the principle of least action, the equilibrium configuration should minimize the potential energy (i.e., it should minimize the above integral); thus, in the absence of any constraint, we see that the membrane is deformed to become a **minimal graph**. If in addition we suppose that the deformation of the membrane is smooth and very small, then

$$S_1 \approx \int_\Omega \left(1 + \frac{1}{2}|Du(x)|^2\right) dx.$$

Therefore, locally, the potential energy of deformation will essentially be $\frac{1}{2}\int_\Omega |Du(x)|^2 dx$. Thus, for simplicity, we define

$$\mathcal{E}(u) = \int_\Omega |Du(x)|^2 dx,$$

which is the integral studied by Dirichlet, Riemann and many others in classical function theory. Minimizers of $\mathcal{E}$ are **harmonic functions**, i.e., they satisfy

$$\Delta u = 0. \tag{2.3}$$

We are yet to incorporate the constraint that the membrane lies above a given obstacle. An anecdotal example goes as follows:

> *The King ordered a hat to be made for himself, fashioned as a minimal garment over a specified ridge.*

A hat like this would resemble an example of a *constrained* minimal surface, as illustrated in Figure 2. Our task would be to find the configuration among

[1] In general, the membrane may also be loaded by an external force, which we ignore here.



Figure 2: AI-generated King's hat.

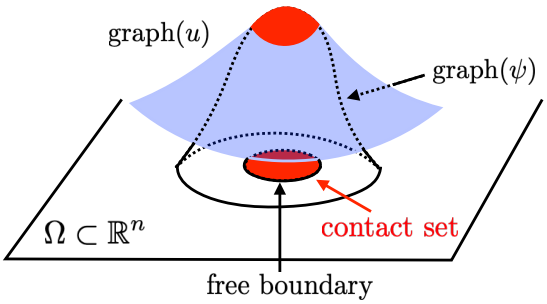


Figure 3: A possible solution to the obstacle problem

all those in (2.2) that minimizes the energy $\mathcal{E}$ subject to the obstacle constraint (the surface should lie above the head of the King).

In order to formulate the constraint mathematically, consider an open set $O \subset \mathbb{R}^{n+1}$, which we call an **obstacle**, and which is of the form

$$O = \{(x, x_{n+1}) : \ x \in \overline{\Omega}, \ x_{n+1} < \psi(x)\},$$

where $\psi : \overline{\Omega} \to \mathbb{R}$ is a given smooth function. Our assumption is that the membrane does not penetrate the obstacle, i.e., $(x, u(x)) \notin O$ or, equivalently, due to our graphical assumptions, that the membrane stays above the obstacle:

$$u(x) \geq \psi(x), \quad x \in \overline{\Omega}. \tag{2.4}$$

Thus, combining (2.2) and (2.4), we define the class of admissible deformations to be

$$\mathbb{K} = \{v \in W_g^{1,2}(\Omega) : \ v(x) \geq \psi(x) \text{ for } x \in \Omega\},$$

where $W_g^{1,2}(\Omega)$ is the space of functions in $L^2(\Omega)$, whose derivatives are also in $L^2(\Omega)$, and which take the boundary value g. We remark that $\mathbb{K}$ may be empty, for instance if $g(x_0) < \psi(x_0)$ for some $x_0 \in \partial\Omega$: in this case the problem becomes trivial.

In short, the obstacle problem is to find the solution $u \in \mathbb{K}$ to the following problem:

$$\mathcal{E}(u) = \min_{v \in \mathbb{K}} \mathcal{E}(v).$$

One can then show that the solution is characterized through the following partial differential equation

$$\Delta u = \Delta\psi \, \chi_{\{u=\psi\}}. \tag{2.5}$$

This equation asserts that when u does not feel the obstacle (i.e., $u > \psi$) then u is harmonic, as in (2.3); and that when u feels the obstacle (i.e., $u = \psi$) we have $\Delta u = \Delta\psi$. Hence (2.5) implies that the equation for $\Delta u(x)$ changes depending on which of the following two sets the point x belongs to:

non-contact set $\{u > \psi\}$, **contact set** $\{u = \psi\}$.

A fundamental feature of the problem is that these sets are not prescribed a priori, and neither is their topological boundary $\partial\{u > \psi\}$, which is therefore called a **free boundary**. See Figure 3 for an illustration.

Provided that $\mathbb{K}$ is non-empty, standard arguments in the Calculus of Variations yield the existence of a generalized solution to the obstacle problem, and so a basic issue is to understand the regularity and geometric properties of such solutions and of their respective free boundaries. This question is typically considered under the assumption that

$$\Delta\psi < 0. \tag{2.6}$$

In the absence of this condition, the free boundary can behave essentially in an arbitrary way [Caf98]. Regarding the regularity of the solution, it has been

known since the 1970s that $u \in C^{1,1}(\Omega)$, which is optimal, as (2.5) and (2.6) imply that the Laplacian of u is discontinuous across the free boundary. Consequently, $u \notin C^2(\Omega)$ in general. On the other hand, analyzing the free boundary is significantly more complex and remains an active area of research.

Generally, free boundaries are singular, even when $n = 2$. Caffarelli [Caf77] showed a powerful dichotomy: when we zoom in around any free boundary point, then

1. either the contact set looks like a half-space (in which case the case the free boundary is smooth around that point, and we say that the free boundary point is "regular");

2. or the contact set is thin (in which case the free boundary point is called "singular").

See Figure 4 for an illustration of either scenario.

It is well-known that singular points are not rare. Actually, the set of singular points may have the same dimension as the set of regular points. One can then ask more refined questions about the structure of the set of singular points.

Caffarelli's result shows that the set of singular points is always *contained* locally in a C^1 manifold. Nonetheless, in specific instances this set can be very wild and display Cantor-like behavior, as was shown by Schaeffer [Sch77]. In fact, he conjectured that, although this type of behavior is unavoidable, it is non-generic: in particular, it should disappear under perturbations of the boundary datum g. This conjecture was confirmed first when $n = 2$ [Mon03] and, more recently, whenever $n \leq 4$ [FROS20]. Thus, in low dimensions, generic free boundaries have no singular points and are therefore smooth.

3 The vectorial obstacle problem

In the previous section we considered graphical deformations of a membrane, see (2.1). We now consider completely general deformations, which we represent as parametric surfaces with a prescribed boundary. It is natural to consider general deformations since,

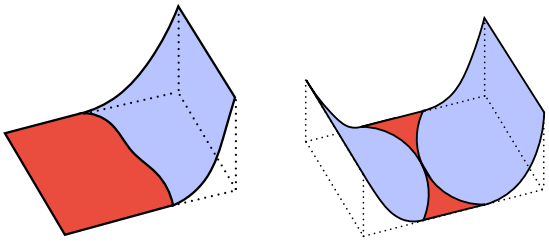


Figure 4: Regular vs singular free boundaries: either the contact set looks like a half-space, or it is thin.

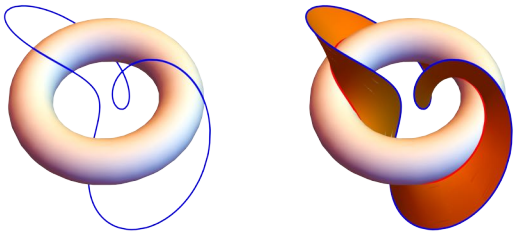


Figure 5: Courant's problem: the given surface is a torus and the prescribed Jordan curve is in blue.

in more complicated geometric situations, the preferable deformation may not be graphical. For a concrete example, consider the following problem from the classical book of Courant [Cou77]:

> *"Find a doubly connected surface of minimal area, one of whose boundaries is free on a given surface, such as a sphere, while the other boundary is a prescribed Jordan curve."*

This is a parametric version of the King's hat-problem defined in the previous section. Clearly, for complicated Jordan curves, it is unreasonable to expect the solution to be a graph, see e.g. Figure 5.

In order to formulate precisely the type of problems that we will consider, let $\Omega \subset \mathbb{R}^n, O \subset \mathbb{R}^m$ be smooth bounded domains and let $\mathbf{g} \in C^\infty(\partial\Omega; \mathbb{R}^m)$ be some

boundary datum. As before, we want to minimize

$$\mathcal{E}(\mathbf{v}) = \int_\Omega |D\mathbf{v}|^2 \, dx \tag{3.1}$$

among all maps $\mathbf{v} = (v^1, \cdots, v^m)$ that coincide with $\mathbf{g}$ on the boundary and which avoid the obstacle O: more precisely, the family of admissible maps is

$$\widetilde{\mathbb{K}} = \{\mathbf{v} \in W^{1,2}_{\mathbf{g}}(\Omega; \mathbb{R}^m) : \mathbf{v}(x) \notin O \text{ for a.e. } x \in \Omega\},$$

which clearly generalizes our previous definition even in the particular case $m = n + 1$. We refer to minimizers of $\mathcal{E}$ in $\widetilde{\mathbb{K}}$ as **minimizing constraint maps**.

As in the scalar case, for any admissible map $\mathbf{v}$ the domain Ω is naturally decomposed into the sets of points which are either mapped to the boundary of the obstacle or to outside the obstacle, together with the free boundary between them:

$$\mathbf{u}^{-1}(\partial O) = \{x \in \Omega : \mathbf{u}(x) \in \partial O\},$$

$$\mathbf{u}^{-1}(\mathbb{R}^m \setminus \overline{O}) = \{x \in \Omega : \mathbf{u}(x) \notin \overline{O}\},$$

$$\mathcal{F}_{\mathbf{u}} = \partial\{x \in \Omega : \mathbf{u}(x) \in \partial O\};$$

see also Figure 7 for an illustration. Given a minimizer $\mathbf{u}$ of $\mathcal{E}$ we can then derive equations similar to (2.5) to find that

$$\Delta \mathbf{u} = \mathcal{A}_{\mathbf{u}}(D\mathbf{u}, D\mathbf{u}) \, \chi_{\mathbf{u}^{-1}(\partial O)} \quad \text{in } \Omega, \tag{3.2}$$

as was done in [Duz87]. Here, $\mathcal{A}$ denotes the second fundamental form of ∂O: $\mathcal{A}_{\mathbf{u}(x)}$ is a quadratic form on the tangent space of ∂O at $\mathbf{u}(x)$ which encodes the curvature of ∂O at that point. For instance, in the model case where O is the ball $B_1(0)$, we have

$$\mathcal{A}_{\mathbf{u}}(D\mathbf{u}, D\mathbf{u}) = -|D\mathbf{u}|^2 \mathbf{u}.$$

Note that (3.2) is a coupled system of m equations, one for each component of $\mathbf{u}$. Moreover, as in (2.5), we have $\Delta \mathbf{u} = 0$ at points where the obstacle is not felt. There is however an important difference compared to (2.5): at points where the obstacle is felt, we have $\Delta u = \Delta \psi$ in the scalar case, while in the vectorial case we have

$$\Delta \mathbf{u} = \mathcal{A}_{\mathbf{u}}(D\mathbf{u}, D\mathbf{u}). \tag{3.3}$$

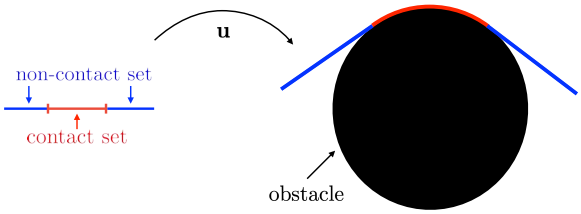


Figure 6: A geodesic in $\mathbb{R}^m \setminus O$.

Thus, unlike in the scalar case, the right-hand side in this equation is not fixed a priori but instead depends nonlinearly on the solution itself: in fact, it can be viewed as a Lagrange multiplier, enforcing the constraint $\mathbf{u} \in \partial O$. Equation (3.3) asserts that $\mathbf{u}$ is a **harmonic map** into ∂O when restricted to the interior of the set $\mathbf{u}^{-1}(\partial O)$.

There is an additional important difference between the scalar and vectorial cases. We saw that, in the scalar case, any minimizer of $\mathcal{E}$ is a solution of (2.5); conversely, it is known that any solution of (2.5) is a minimizer of $\mathcal{E}$. However, this is not true in the vectorial setting: while minimizers are indeed solutions of (3.2), the converse no longer holds. In fact, there are fundamental differences between minima and general solutions of the differential equations.

We now overview some of the history and fundamental examples of minimizing constraint maps:

1. When $n = 1$, (3.2) becomes a system of ordinary differential equations. In this case, minimizing constraint maps are simply unit-speed parametrizations of minimizing **geodesics** in the manifold-with-boundary $\mathbb{R}^m \setminus O$, see Figure 6. Note that, even in this case, a solution of the differential equations (i.e., a geodesic in $\mathbb{R}^m \setminus O$) is not necessarily minimizing.

2. The case $n = 2$ is very classical and was studied by Morrey [Mor48] (for harmonic maps) and then by Hildebrandt [Hil72] and Tomi [Tom71] (for constraint maps). Among other things, they proved that minimizing constraint maps are $C^{1,\alpha}$, for any $\alpha \in (0, 1)$.

3. When $n \geq 3$, the theory of minimizing constraint

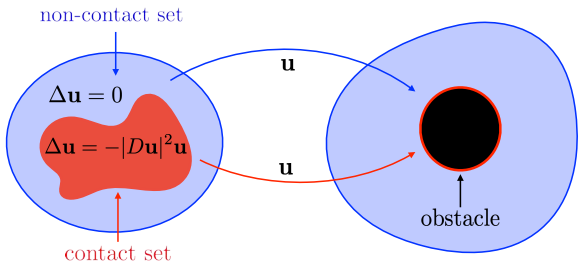


Figure 7: An obstacle that forces discontinuities.

maps becomes especially rich: even in the simplest possible setting where $n = m \geq 3$, $\mathbf{g} = \mathbf{id}$ and $\Omega = B_1(0)$, $O = B_{1/2}(0)$, minimizing constraint maps develop **discontinuities**. Indeed, as it is apparent from Figure 7, one has to dissect and break apart $B_1(0)$ to fit it onto the target set; this can be made precise using tools from Algebraic Topology and, in particular, degree theory. Here, the condition $n = m \geq 3$ is only used to guarantee that the class of admissible maps is non-empty, since it contains the map $\mathbf{u}_*(x) = x/|x|$, and so an actual minimizing constraint map exists. When $n = m = 2$ the map $\mathbf{u}_*$ has infinite Dirichlet energy: in fact, this holds more generally for any map $\mathbf{u}\colon B_2(0) \to \mathbb{R}^2 \setminus B_1(0)$ with $\mathbf{u} = \mathbf{id}$ on $\partial B_2(0)$, as can be seen using the refined degree theory of Brezis and Nirenberg. We shall henceforth write

$$\Sigma_{\mathbf{u}} = \{x \in \Omega : \mathbf{u} \text{ is discontinuous at } x\}.$$

Starting from the seminal work of Schoen and Uhlenbeck [SU82], it was shown in [DF86, Luc88, FKS24] that

$$\mathbf{u} \in C^{1,1}_{\mathrm{loc}}(\Omega \setminus \Sigma_{\mathbf{u}}), \qquad \dim \Sigma_{\mathbf{u}} \leq n - 3, \quad (3.4)$$

a result which is, in general, optimal. Thus, although discontinuities are inevitable, they form a rather small set. We note that, in special circumstances, discontinuities may not be present at all: this is the case, for instance, whenever the obstacle is graphical [FW89].

It is worth explaining in more detail the tools used in the proof of (3.4). The main idea, which is standard in this type of problems, is to understand the behavior of a minimizing constraint map $\mathbf{u}$ around a point $x_0 \in \Omega$ by studying rescalings of $\mathbf{u}$, more precisely

$$\mathbf{u}_{x_0,r}(x) := \mathbf{u}(x_0 + rx)$$

for $r > 0$. Thus, as $r \searrow 0$, $\mathbf{u}_{x_0,r}$ resembles an increasingly zoomed-in version of $\mathbf{u}$. The result (3.4) follows in a standard way from the following three fundamental properties of these rescalings:

- **Monotonicity formula:** the rescaled energy

$$E(\mathbf{u}, x_0, r) := r^{2-n} \int_{B_r(x_0)} |D\mathbf{u}|^2 dx$$

is a non-decreasing function of r, and it is constant if and only if $\mathbf{u}_{x_0,r}(x) = \mathbf{u}(x_0 + x)$ for all x and all $r > 0$. Note also that $E(\mathbf{u}, x_0, r) = E(\mathbf{u}_{x_0,r}, 0, 1)$, thus the energy is rescaled according to the rescalings of $\mathbf{u}$.

- **Compactness:** the sequence of rescalings $\{\mathbf{u}_{x_0,r}(x)\}_{r>0}$ is pre-compact in $W^{1,2}$: if $r_j \searrow 0$ then there is a new subsequence $r_{j'} \searrow 0$ and a minimizing constraint map $\boldsymbol{\phi}\colon \mathbb{R}^n \to \mathbb{R}^m \setminus O$ such that

$$D\mathbf{u}_{x_0,r'_j} \to D\boldsymbol{\phi} \quad \text{in } L^2_{\mathrm{loc}}(\mathbb{R}^n).$$

By the monotonicity formula, $\boldsymbol{\phi}$ is 0-homogeneous, i.e., $\boldsymbol{\phi}(rx) = \boldsymbol{\phi}(x)$ for all $x \in \mathbb{R}^n$, all $r > 0$.

- **ε-regularity theorem:** there is $\varepsilon > 0$ such that

$$E(\mathbf{u}, x_0, r) \leq \varepsilon \quad \Longrightarrow \quad \mathbf{u} \in C^{1,1}(B_{r/2}(x_0)),$$

with a corresponding estimate. Thus $\mathbf{u}$ is regular around points of small normalized energy and, conversely,

$$\Sigma_{\mathbf{u}} = \left\{ x_0 \in \Omega : \lim_{r \to 0} E(\mathbf{u}, x_0, r) > 0 \right\}.$$

By the compactness result, we also have $x_0 \in \Sigma_{\mathbf{u}}$ if and only if there is a sequence $r_j \searrow 0$ such that $D\mathbf{u}_{x_0,r_j} \to D\boldsymbol{\phi}$ in L^2_{loc}, for some non-constant map $\boldsymbol{\phi}$.

The results above provide a broad overview of the regularity theory for minimizing constraint maps, paralleling the regularity theory of harmonic maps. However, they leave many fundamental questions unanswered. For instance, how does the geometry of the obstacle O interact with the discontinuity set? And what can be understood about the structure and regularity of the associated free boundaries? We will explore these questions in the following sections.

4 Discontinuities vs free boundaries

As we have seen, even in very simple situations, minimizing constraint maps develop discontinuities. Such discontinuities must necessarily lie within the closure of the contact set $\mathbf{u}^{-1}(\partial O)$, since in the non-contact set we have $\Delta \mathbf{u} = 0$ by (3.2), making $\mathbf{u}$ smooth there. A natural question, then, is whether $\mathbf{u}$ can have discontinuities on the free boundary or if they are confined to the interior of $\mathbf{u}^{-1}(\partial O)$.

The above question is of course only meaningful if a free boundary actually occurs, and this happens only when Ω is mapped into a part of ∂O with positive curvature. Indeed, Duzaar [Duz87] showed that if ν is the outward unit normal to ∂O, then

$$\mathcal{A}_{\mathbf{u}}(D\mathbf{u}, D\mathbf{u}) \cdot (\nu \circ \mathbf{u}) \leq 0 \quad \text{ on } \mathbf{u}^{-1}(\partial O). \tag{4.1}$$

If τ is a principal direction of ∂O with corresponding principal curvature κ, then $\mathcal{A}_y(\tau, \tau) \cdot \nu_y = -\kappa(y)$. Thus (4.1) asserts that $\mathbf{u}$ may only touch ∂O at points where ∂O satisfies a convexity-type condition (when seen from O): indeed, this inequality always holds if O is convex, a case where we can then expect free boundaries to occur. Note however that (4.1) is subtle, as it depends on $\mathbf{u}$ itself. For instance, if $D\mathbf{u}$ vanishes at a point then (4.1) holds at that point, regardless of the geometry of O. We will return to this situation in Section 5 below.

The above discussion suggests that we should consider **convex obstacles** in order to hope for a reasonable answer to our question. In [FGKS23, FGKS24] we showed that indeed the convexity condition leads to some good properties of constraint maps:

Theorem 1. *Let $\mathbf{u}\colon \Omega \to \mathbb{R}^m \setminus O$ be a minimizing constraint map, where we assume that*

$$O \text{ is convex.}$$

Then the function $x \mapsto \operatorname{dist}(\mathbf{u}(x), O)$ is continuous.

In particular, Theorem 1 guarantees that, for convex obstacles, the non-contact set

$$\mathbf{u}^{-1}(\mathbb{R}^m \setminus O) = \{\operatorname{dist}(\mathbf{u}, O) > 0\}$$

is well-defined and open.

We now provide a sketch of the proof of Theorem 1. Since $\operatorname{dist}(\mathbf{u}, O)$ is continuous at points where $\mathbf{u}$ is continuous, it suffices to establish the continuity of $\operatorname{dist}(\mathbf{u}, O)$ at the discontinuity points of $\mathbf{u}$. For any such point, say $x_0 \in \Sigma_{\mathbf{u}}$, as shown in the previous section, there exists a non-constant, minimizing constraint map $\boldsymbol{\phi}$ that is 0-homogeneous and arises as the limit of a sequence of rescalings $\mathbf{u}_{x_0,r}$. As $\boldsymbol{\phi}$ is itself a solution of the Euler–Lagrange system (3.2) and, as O is convex, we have that the function

$$x \mapsto \operatorname{dist}(\boldsymbol{\phi}(x), O) \quad \text{ is subharmonic.}$$

Since this function is also 0-homogeneous, by the maximum principle it must be constant. In fact, we must have

$$\operatorname{dist}(\boldsymbol{\phi}, O) = 0,$$

for otherwise $\boldsymbol{\phi}$ would never touch ∂O and so we would have $\Delta \boldsymbol{\phi} = 0$, which is impossible since $\boldsymbol{\phi}$ is 0-homogeneous and non-constant. Now, according to the definition of the rescalings, we have

$$\begin{aligned} \|\operatorname{dist}(\mathbf{u}, O)\|_{L^2(B_r(x_0))} &= \|\operatorname{dist}(\mathbf{u}_{x_0,r}, O)\|_{L^2(B_1(0))} \\ &\to \|\operatorname{dist}(\boldsymbol{\phi}, O)\|_{L^2(B_1(0))} = 0, \end{aligned}$$

as $r \to 0$, since $\mathbf{u}_{x_0,r} \to \boldsymbol{\phi}$ in L^2_{loc}. To conclude that $\operatorname{dist}(\mathbf{u}, O)$ is continuous at x_0, it suffices to upgrade the above L^2-convergence to L^∞-convergence. Since $\operatorname{dist}(\mathbf{u}, O)$ is subharmonic (due to the convexity of O), the L^2-norm controls the L^∞-norm by the mean value property.

Note that we may always decompose a map $\mathbf{u}\colon \Omega \to \mathbb{R}^m \setminus O$ in its normal and tangential components (with respect to O); explicitly, we have

$$\mathbf{u} = \operatorname{dist}(\mathbf{u}, O)(\nu \circ \Pi \circ \mathbf{u}) + \Pi \circ \mathbf{u},$$

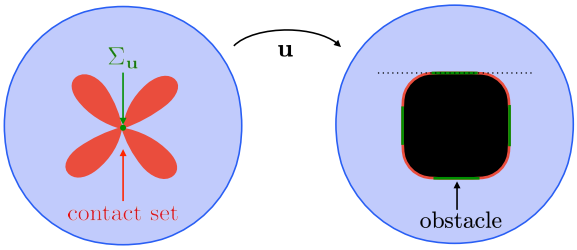


Figure 8: A convex obstacle with flat sides forces discontinuities on the free boundary: the discontinuity points are mapped to the flat sides.

where as before ν is the outwards unit normal to O and $\Pi\colon \mathbb{R}^m \setminus O \to \partial O$ is the nearest point projection. Theorem 1 shows that the components of $\mathbf{u}$ normal to O are continuous, but what about the tangential components? Surprisingly, in [FGKS24] we observed that the tangential components are in general discontinuous on the free boundary:

Theorem 2. *Let $n = m$ and $\Omega = B$ be a ball. There exists a convex obstacle O such that the energy-minimizing map $\mathbf{u}\colon \Omega \to \mathbb{R}^n \setminus O$ has the property that*

$$\Sigma_{\mathbf{u}} \cap \mathcal{F}_{\mathbf{u}} \neq \emptyset.$$

The obstacles in Theorem 2 are easy to describe: any convex obstacle with **flat pieces** (i.e. an obstacle which contains a portion of a hyperplane in $\mathbb{R}^m$) will induce discontinuities on the corresponding free boundaries, provided that

$$\overline{O} \subset \Omega = B, \qquad \mathbf{u} = \mathbf{id} \text{ on } \partial\Omega, \tag{4.2}$$

see Figure 8. This is somewhat counter-intuitive: when the obstacle is a half-space we have $\mathcal{A} = 0$; so minimizing constraint maps are simply solutions of $\Delta \mathbf{u} = 0$ and, in particular, they are analytic.

We now explain the mechanism behind Theorem 2. Suppose there is a free boundary point $x_0 \in \mathcal{F}_{\mathbf{u}}$ that is a continuity point of $\mathbf{u}$ and which is mapped to a flat piece $P \subset \partial O$. Any such flat piece can be characterized by a linear equation; for simplicity, let us say

$$P = \{\mathbf{y} = (y^1, \dots, y^n) : y^n = \tfrac{1}{2}\} \cap O,$$

and assume that $\{y^n \geq \frac{1}{2}\} \subset \mathbb{R}^n \setminus O$, see Figure 8. By continuity of $\mathbf{u}$ at x_0, we can find a small radius $r > 0$ such that

$$\mathbf{u}(B_r(x_0) \cap \mathbf{u}^{-1}(\partial O)) \subset P.$$

Since $\mathcal{A} = 0$ in P, it follows from (3.2) that $\Delta \mathbf{u} = 0$ in $B_r(x_0)$. Thus

$$\Delta u^n = 0 \text{ and } u^n \geq \tfrac{1}{2} \text{ in } B_r(x_0), \quad u^n(x_0) = \tfrac{1}{2}.$$

The maximum principle for harmonic functions forces $u^n = \frac{1}{2}$ in $B_r(x_0)$. Since $\Delta \mathbf{u} = 0$ in the non-contact set $\mathbf{u}^{-1}(\mathbb{R}^n \setminus O)$ and the latter is connected, the unique continuation property of harmonic functions implies that $u^n = \frac{1}{2}$ throughout the entire non-contact set (recall that harmonic functions are analytic). This, of course, contradicts our choice of boundary conditions in (4.2). Thus, $\mathbf{u}$ cannot continuously map a free boundary point into a flat piece.

The main challenge is thus to prove the existence of a free boundary point that is mapped to a flat piece. In fact, one can prove that (4.2) forces $\mathbf{u}$ to fill the annulus $\Omega \setminus O$, i.e. we must have

$$\mathbf{u}(\Omega) = \Omega \setminus O$$

in order to minimize the amount of "breaking" occurring in Ω. As a consequence, there must be free boundary points that are mapped to a flat piece, and these points are necessarily discontinuities. To prove that $\mathbf{u}$ is onto the annulus, the key step is to show that $\mathbf{u}$ is a local diffeomorphism in a neighborhood of $\partial\Omega$, so that the rank of the boundary map is preserved close to $\partial\Omega$. Once this is proved, the surjectivity follows from degree theory.[2] To prove that our map is a local diffeomorphism in a neighborhood of the prescribed boundary, we require a combination of analytical and geometric tools, such as the maximum principle, and the unique continuation property of harmonic functions.

It is an interesting problem to understand the geometry of the contact set $\mathbf{u}^{-1}(\partial O)$ for the above example. We refer the reader to Figure 8 for a suggestion of what it may look like; we emphasize however

[2] We do not know how to avoid the use of degree theory in the proof of the surjectivity of $\mathbf{u}$ onto the annulus.

that we do not yet know if the free boundary is singular at points in $\Sigma_{\mathbf{u}} \cap \mathcal{F}_{\mathbf{u}}$. The argument above suggests that $\mathbf{u}$ should map a single free boundary point to an entire flat piece of ∂O. Therefore, there may be a singular point in $\mathcal{F}_{\mathbf{u}}$ for each flat piece of ∂O, or there could be a singular point in $\mathcal{F}_{\mathbf{u}}$ that is mapped simultaneously to different flat pieces.

Theorems 1 and 2 give a rather complete picture of what happens for general convex obstacles. However, in the scalar obstacle problem, where $\mathcal{A}$ is replaced by $\Delta\psi$ for some prescribed function ψ, one typically assumes the quantitative condition (2.6). Thus it is natural to wonder whether a more quantitative version of convexity, such as **uniform convexity**, leads to better results. We recall that O is said to be uniformly convex if all of the principal curvatures of ∂O are positive and bounded away from zero: essentially, O looks "round". In [FGKS24], we obtained the following positive result:

Theorem 3. *Let $\mathbf{u}\colon \Omega \to \mathbb{R}^m \setminus O$ be a minimizing constraint map, where we assume that*

$$O \text{ is } \textbf{\textit{uniformly}} \text{ convex.}$$

There exists $\delta > 0$ such that

$$x \in \Sigma_{\mathbf{u}} \quad \Longrightarrow \quad \delta \leq \operatorname{dist}(x, \mathcal{F}_{\mathbf{u}}).$$

In other words, that are no discontinuities on the free boundary.

The proof of Theorem 3 is unfortunately too technically involved to describe in detail here. In essence, the uniform convexity of O allows for a quantification of the proof of Theorem 1 described above, but it requires many new ideas. The proof integrates concepts from De Giorgi regarind subsolutions of elliptic equations, the frequency function introduced by Almgren in the study of minimal surfaces, and the identification of a critical scale which separates precisely the regions of regular and irregular behavior of $\mathbf{u}$, in line with the recent work of Naber and Valtorta [NV17].

5 Branch points and singular free boundaries

In the scalar obstacle problem, a successful regularity theory for free boundaries was built under the quantitative assumption (2.6). The scalar theory can be applied to study the regularity of free boundaries also in the vectorial setting, provided that the right-hand side in (3.2) is non-degenerate, the relevant quantity here being

$$F(\mathbf{u})(x) := \operatorname{Hess}\left(\operatorname{dist}(\cdot, O)\right)_{\mathbf{u}(x)} [D\mathbf{u}, D\mathbf{u}] \geq 0,$$

where the last inequality holds whenever O is convex. It is not surprising that the Hessian of the distance to O is relevant here, since such a quantity is closely related to the second fundamental form of ∂O.

Essentially, whenever $F(\mathbf{u}) > 0$, condition (2.6) holds and the scalar theory is applicable [FKS24]. There are two important cases, however, where this condition cannot hold:

1. at discontinuity points of $\mathbf{u}$, then $|F(\mathbf{u})| = \infty$;
2. at points where $D\mathbf{u} = 0$, then $F(\mathbf{u}) = 0$.

Thus, in both cases, the scalar theory is entirely inapplicable. In the previous section, we provided a comprehensive overview of how the geometry of the obstacle interacts with the existence of discontinuity points on free boundaries. We will now turn our attention to discussing the set of points where

$$D\mathbf{u} = 0.$$

We refer to that set as the set of **branch points**.

There are two distinct yet intriguing aspects of branch points. Firstly, if branch points exist on a free boundary, they may significantly affect its regularity, as the vectorial obstacle problem becomes degenerate at these points. We will discuss this aspect in detail shortly. Secondly, at a branch point, one cannot apply the Implicit Function Theorem to $\mathbf{u}$. Thus, if we consider $\mathbf{u}$ as a parametrization of its image $\mathbf{u}(\Omega)$, the image itself may develop singularities.

Let us illustrate this second point in a simple but compelling example, which will also clarify how our

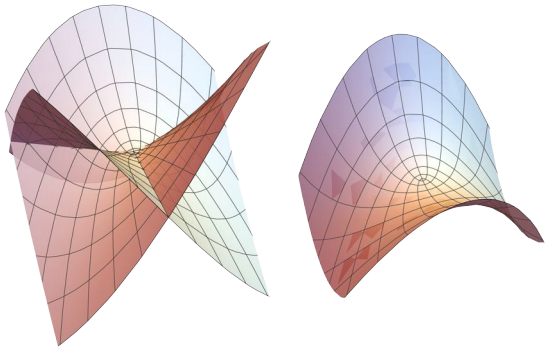


Figure 9: $\mathbf{u}_k(\mathbb{R}^2)$ for $k = 3$ (left) and $k = 4$ (right).

notion of branch point is related to analogue concepts in classical function theory and in the theory of parametric minimal surfaces. Consider, for $k \in \mathbb{N}$, the maps $\mathbf{u}_k \colon \mathbb{C} \cong \mathbb{R}^2 \to \mathbb{R}^3$ defined by

$$\mathbf{u}_k(z) = (z^2, \operatorname{Re} z^k), \quad z \in \mathbb{C},$$

whose images are depicted in Figure 9. Notice that 0 is a branch point of $\mathbf{u}_k$ (and it is, in fact, the only such point). There is an interesting difference between the case where k is odd and k is even: in the former, there is an actual singularity of $\mathbf{u}(\mathbb{R}^2)$ at 0; in the latter, the parametrization $\mathbf{u}$ is degenerate at 0, but the surface $\mathbf{u}(\mathbb{R}^2)$ is perfectly smooth.

The maps $\mathbf{u}_k$ clearly satisfy $\Delta \mathbf{u}_k = 0$, and so they are minimizers of the Dirichlet energy (3.1), without any constraints on the image of the competitors. In particular, they are also minimizing constraint maps for any obstacle $O \subset \mathbb{R}^3$ such that

$$O \subset \mathbb{R}^3 \setminus \overline{\mathbf{u}_k(\mathbb{R}^2)}.$$

By choosing appropriate sets O, one can produce simple but interesting examples of branch points on free boundaries, as the reader can see in Figure 10. The case where k is odd is especially interesting: as in Figure 10, for any such k one can construct a non-convex obstacle of class $C^{(k-1)/2}$ such that the free boundary is a cone with tip at the branch point at 0.

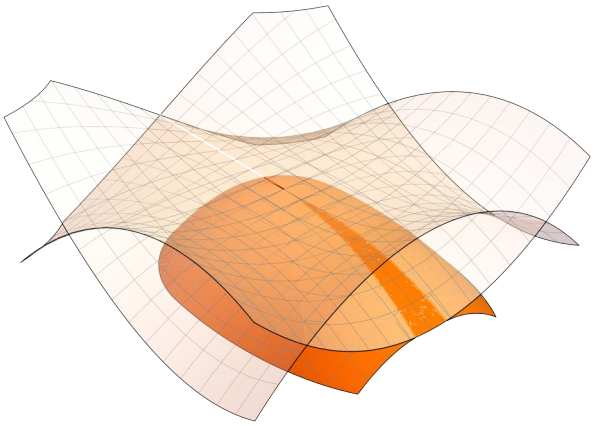


Figure 10: An artificial obstacle touching the image of $\mathbf{u}_5$ over a cone with tip at 0. Note that the obstacle is not convex but that it is of class $C^{2,1/2}$.

The type of free boundary singularities depicted in Figure 10 cannot occur in the scalar obstacle problem under the quantitative condition (2.6), as per Caffarelli's dichotomy. As the above obstacle is not even convex, and in light of the positive results of Theorem 3, it is natural to ask what happens for uniformly convex obstacles: can the free boundary prevent branching?

It turns out that, even in very simple situations, the answer is no, even when the obstacle is the unit ball $\mathbb{B}^3 \subset \mathbb{R}^3$:

Theorem 4. *There is a minimizing constraint map* $\mathbf{u} \colon \Omega \to \mathbb{R}^3 \setminus \mathbb{B}^3$ *such that*

$$\{D\mathbf{u} = 0\} \cap \mathcal{F}_{\mathbf{u}} \neq \emptyset,$$

and the free boundary $\mathcal{F}_{\mathbf{u}}$ *is singular at such points.*

The geometric idea behind Theorem 4 is simple to explain. In doing so, we will also provide a more detailed version of the result, including a more precise description of the nature of the singularities of the free boundary.

For a fixed integer $k \in \mathbb{N}$, we consider k-axially symmetric maps $\mathbf{u} \colon \mathbb{B}^3 \to \mathbb{R}^3 \setminus \mathbb{B}^3$. Specifically, in cylindrical coordinates (r, θ, x_3) and $\mathbf{u} = (u^r, u^\theta, u^3)$

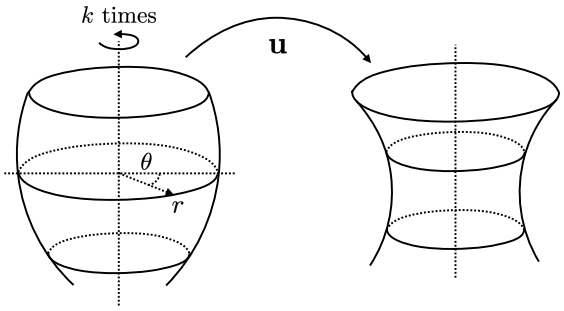


Figure 11: A k-axially symmetric map $\mathbf{u}$ maps horizontal circles centered on the vertical axis to other such circles, while rotating each of them k-times.

for both the domain and the target, we have

$$\mathbf{u}(r,\theta,x_3) = \left(u^r(r,x_3), k\theta, u^3(r,x_3)\right).$$

In other words, $\mathbf{u}$ maps each horizontal circle centered on the vertical axis to another such circle, while rotating it k times, see Figure 11. Given any non-trivial k-axially symmetric boundary condition, for instance

$$\mathbf{g}(r,\theta,x_3) = (r, k\theta, x_3),$$

we then minimize the Dirichlet energy (3.1) among k-axially symmetric maps taking values in $\mathbb{R}^3\backslash\mathbb{B}^3$ which agree with g on $\partial\mathbb{B}^3$. Although the resulting map $\mathbf{u}$ is not necessarily a minimizing constraint map, it can be shown that it is in fact minimizing around any of its continuity points. In particular, by (a variant of) Theorem 3, $\mathbf{u}$ is minimizing in a neighborhood of any free boundary point, which is the region that concerns us.

Let us now take a point on the vertical axis. Our construction is based on the following simple observation: if $k \geq 2$ and $\mathbf{u} = (u^1, u^2, u^3)$ is a k-axially symmetric map, then

$$Du^1(0,0,x_3) = Du^2(0,0,x_3) = 0, \qquad (5.1)$$

provided that $\mathbf{u}$ is C^1 around $(0,0,x_3)$. Indeed, since $\mathbf{u}$ rotates at least twice about the vertical axis, the only way it can do so in a regular manner is by having vanishing gradient on this axis. Now suppose, in addition, that $(0,0,x_3) \in \mathcal{F}_{\mathbf{u}}$ is a free boundary point.

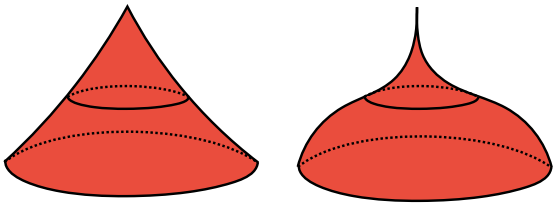


Figure 12: At a branch point, the contact set either looks like a cone or like the vertical axis. In either case, the free boundary is singular.

Then $|\mathbf{u}|(0,0,x_3) = 1$, and since $|\mathbf{u}| \geq 1$ and $|\mathbf{u}|$ is smooth around $(0,0,x_3)$, we have

$$0 = D|\mathbf{u}|(0,0,x_3) = Du^3(0,0,x_3),$$

where we used also (5.1) in the last equality. We conclude that *any free boundary point on the vertical axis is a branch point.*

What does the free boundary look like near such a point? Since we are in the axially symmetric setting, we can compute many things fairly explicitly. In [FGKS24], we showed that, as we zoom in around a free boundary point on the vertical axis, the free boundary either looks like a cone or like the vertical axis, see Figure 12. In the former case, the angle of the cone is quantized: if φ is the angle between the cone and the vertical axis, then $\cos(\varphi)$ must be a zero of the Legendre polynomial of order $2k-1$, where k is the number of times $\mathbf{u}$ wraps around the vertical axis. In either case, we see that the free boundary is singular at such a point. An interesting problem is to understand whether both types of singularities are actually possible: in our analysis we can only show that the free boundary looks like one of the two scenarios in Figure 12, but we do not know whether both may occur in practice. Recall that cone-like singularities cannot occur in the scalar obstacle problem (cf. Figure 4). If they occur in this context, they represent a genuinely vectorial feature resulting from the emergence of branch points.

Acknowledgements

A.F. has been partially supported by the European Research Council under the Grant Agreement No. 721675 "Regularity and Stability in Partial Differential Equations (RSPDE)". A.G. was supported by Dr. Max Rössler, the Walter Haefner Foundation, and the ETH Zürich Foundation. S.K. was supported by a grant from the Verg Foundation. H.S. was supported by the Swedish Research Council (grant no. 2021-03700).

Declarations

Data availability statement: All data needed are contained in the manuscript.

Funding and/or Conflicts of interests/Competing interests: The authors declare that there are no financial, competing or conflict of interests.

References

[Caf98] L. A. Caffarelli, *The obstacle problem revisited*, J. Fourier Anal. Appl. **4** (1998), no. 4-5, 383–402. MR1658612

[Caf77] ———, *The regularity of free boundaries in higher dimensions*, Acta Math. **139** (1977), no. 1, 155–184. MR0454350

[Cou77] R. Courant, *Dirichlet's Principle, Conformal Mapping, and Minimal Surfaces*, Springer, New York, NY, 1977. MR0454858

[DF86] F. Duzaar and M. Fuchs, *Optimal regularity theorems for variational problems with obstacles*, Manuscripta Math. **56** (1986), no. 2, 209–234. MR0850371

[Duz87] F. Duzaar, *Variational inequalities and harmonic mappings*, J. fur die Reine und Angew. Math. **1987** (1987), no. 374, 39–60. MR0876220

[FGKS23] A. Figalli, A. Guerra, S. Kim, and S. Shahgholian, *Constraint maps with free boundaries: the Bernoulli case*, to appear in J. Eur. Math. Soc. (2023), available at `arXiv:2311.03006`.

[FGKS24] ———, *Constraint maps: singularities vs free boundaries* (2024), available at `arXiv:2407.21128`.

[FKS24] A. Figalli, S. Kim, and H. Shahgholian, *Constraint Maps with Free Boundaries: the Obstacle Case*, Arch. Ration. Mech. Anal. **248** (2024), no. 5, 36pp. MR4795019

[FROS20] A. Figalli, X. Ros-Oton, and J. Serra, *Generic regularity of free boundaries for the obstacle problem*, Publ. Math. IHÉS **132** (2020), no. 1, 181–292. MR4179834

[FW89] M. Fuchs and M. Wiegner, *The regularity of minima of variational problems with graph obstacles*, Arch. der Math. **53** (1989), no. 1, 75–81. MR1005172

[Ger16] J. D. Gergonne, *Questions proposées*, Ann. Math. Pure Appl. **7** (1816), no. 68, 99–100. MR1555884

[Hil72] S. Hildebrandt, *On the regularity of solutions of two-dimensional variational problems with obstructions*, Commun. Pure Appl. Math. **25** (1972), no. 4, 479–496. MR0305178

[Luc88] S. Luckhaus, *Partial Hölder continuity for minima of certain energies among maps into a Riemannian manifold*, Indiana Univ. Math. J. **37** (1988), no. 2, 349–367. MR0963506

[Mon03] R. Monneau, *On the number of singularities for the obstacle problem in two dimensions*, J. Geom. Anal. **13** (2003), no. 2, 359–389. MR1967031

[Mor48] C. B. Morrey, *The Problem of Plateau on a Riemannian Manifold*, Ann. Math. **49** (1948), no. 4, 807. MR0027137

[NV17] A. Naber and D. Valtorta, *Rectifiable-Reifenberg and the regularity of stationary and minimizing harmonic maps*, Ann. Math. **185** (2017), no. 1, 131–227, available at `1504.02043`. MR3583353

[Sch77] D. Schaeffer, *Some examples of singularities in a free boundary*, Ann. Sc. norm. super. Pisa - Cl. sci. **4** (1977), no. 1. MR0516201

[Sch72] H. A. Schwarz, *Fortgesetzte untersuchungen über specielle minimalflächen*, Buchdruckerei der Königlichen Akademie der Wissenschaften (1872), 126–148.

[SU82] R. Schoen and K. Uhlenbeck, *A regularity theory for harmonic maps*, J. Differ. Geom. **17** (1982), no. 2, 307–335. MR0664498

[Tom71] F. Tomi, *Minimal surfaces and surfaces of prescribed mean curvature spanned over obstacles*, Math. Ann. **190** (1971), no. 3, 248–264. MR0271802